PRAMANA
— journal of
physics

Vol. 58, Nos 5 & 6
May & June 2002
pp. 827–837

Novel charge density wave transition in crystals of $R_5Ir_4Si_{10}$

S RAMAKRISHNAN
Tata Institute of Fundamental Research, Homi Bhabha Road, Mumbai 400 005, India
Email: ramky@tifr.res.in

Abstract. We review the observation of novel charge density wave (CDW) transitions in ternary $R_5Ir_4Si_{10}$ compounds. A high quality single crystal of $Lu_5Ir_4Si_{10}$ shows the formation of a commensurate CDW along c-axis below 80 K in the (h, 0, l) plane that coexists with BCS type superconductivity below 3.9 K. However, in a single crystal of $Er_5Ir_4Si_{10}$, one observes the development of a 1D-incommensurate CDW at 155 K, which then locks into a purely commensurate state below 55 K. The well-localized Er^3 moments are antiferromagnetically ordered below 2.8 K which results in the coexistence of strongly coupled CDW with local moment antiferromagnetism in $Er_5Ir_4Si_{10}$. Unlike conventional CDW systems, *extremely sharp transition* (width $\sim$ 1.5 K) in all bulk properties along with huge heat capacity anomalies in these compounds makes this CDW transition an interesting one.

Keywords. Charge density waves; superconductivity; magnetism.

PACS No. 2.0

1. Introduction

For the past two decades, we have witnessed intensive efforts to understand the CDW ordering in low dimensional conductors such as transition-metal dichalcogenides and trichalcogenides [1,2]. Many models [3] have been put forth to explain this transition as due to low dimensionality of these compounds which produces anisotropic Fermi surfaces with small curvature that are favorable for nesting and this leads to the CDW formation. This idea reduces the likelihood of a CDW state in 3-D compounds since the nesting of their Fermi surfaces are difficult due their large curvature (less anisotropy). However, CDW ordering has also been established in 3-D materials such as α-U [4], CuV_2S_4 [5] and $Ba_{1-x}K_xBiO_3$ [6], where the first two are conductors and the last one is an insulator. It appears that in these materials the Fermi surface has an unusual structure which favors nesting although the crystalline anisotropy is small or even absent. However, in order to probe the theory further and search for novel CDW behaviors, especially those involving the interplay with magnetism, new classes of materials are needed. To the best of our knowledge there does not exist a localized moment magnetic system exhibiting a CDW. We have begun a quest for new CDW systems in intermetallic rare-earth (RE) compounds and found indications in [7–9] for such behavior in a series of $R_5Ir_4Si_{10}$ materials. Polycrystalline samples showed anomalies in the resistivity above 20 K, which were tentatively

attributed to CDW or SDW formation [8,9]. In this work, we review the observation of a novel CDW transition in single crystals of $Lu_5Ir_4Si_{10}$ and $Er_5Ir_4Si_{10}$. A high quality single crystal of $Lu_5Ir_4Si_{10}$ shows the formation of superlattice peaks along c-axis below 80 K in the $(h, 0, l)$ plane which can be indexed as $(h, o, l + q)$ where $q = m/7$ and $m = 1, 2, 3, 4, 5, 6$. This sharp commensurate CDW transition coexists with BCS type superconductivity below 3.9 K. On the other hand, in a single crystal of $Er_5Ir_4Si_{10}$, one observes the development of a 1D-incommensurate CDW at 155 K, which then locks into a purely commensurate state below 55 K. The positions of these super lattice reflections can be described by modulation wave vectors $q_1 = (0, 0, 1/4\delta)$, $q_2 = (0, 0, 1/4+\delta)$ and $q_3 = (0, 0, 1/2)$. Further, the development of the incommensurate peaks beginning at 155 K are found to merge into a commensurate $q = (0, 0, 1/4)$ single peak at 55 K. The well-localized Er^3 moments are antiferromagnetically ordered below 2.8 K. Our data suggest the coexistence of strongly coupled CDW with local moment antiferromagnetism in $Er_5Ir_4Si_{10}$. The $R_5Ir_4Si_{10}$ compounds are low anisotropic 3-D compounds which have no chains or layers that are present in canonical CDW systems such as $NbSe_3$ and $NbSe_2$. The sharp CDW transitions in single crystals of $R_5Ir_4Si_{10}$ arise due to unusual nesting of the Fermi surface. *The fact that such sharp features have not been observed even in canonical CDW systems* (*i.e*. $NbSe_3$ *or* $NbSe_2$) *makes this transition an interesting one.* $Lu_5Ir_4Si_{10}$ and $Er_5Ir_4Si_{10}$ adopt tetragonal $Sc_5Co_4Si_{10}$ (P4/mbm) [10] structure where compounds incorporate traditionally 3d magnetic elements such as Co but retaining their superconducting properties. It turns out that in these compounds, the 3*d* elements apparently have no magnetic moment on them. However, they participate in building up a high density of states at the Fermi level which is responsible for the superconductivity [11,12]. Earlier studies on polycrystalline compounds [8,9] have indicated the possibility of CDW formation in $R_5Ir_4Si_{10}$ (R = Dy, Er, Ho, Yb, Tm and Y) series. In this work, we review resistivity (2 to 300 K), magnetization (2 to 300 K), heat capacity (2 to 100 K) and X-ray measurements on a high quality single crystal of $Lu_5Ir_4Si_{10}$ and $Er_5Ir_4Si_{10}$.

2. Experimental

The crystals are made with high purity ($\geq$99.99%) elements in a tri-arc furnace using Czochralski technique. The high quality of the crystal is ascertained using EPMA (JEOL 8600 series, Japan) and the lattice constants are measured using single crystal X-ray diffraction. The structure of $R_5Ir_4Si_{10}$ is shown in figure 1. The interesting structural feature of this compound is the absence of direct transition–transition metal contacts. The transition metal atoms are connected to each other either through R or Si atom. One can observe that Lu has three inequivalent sites. The Ir and Si atoms form planar nets of pentagons and hexagons which are stacked parallel to the basal plane and connected along c-axis via Ir–Si–Ir zigzag chains. The pentagon and hexagon layers are separated by layers of Lu. The distances between Ir and Si as well as Si and Si are short indicating strong covalent interaction. Looking at this structure at 300 K, one has no direct clue about the possibility of CDW in $R_5Ir_4Si_{10}$ at low temperatures.

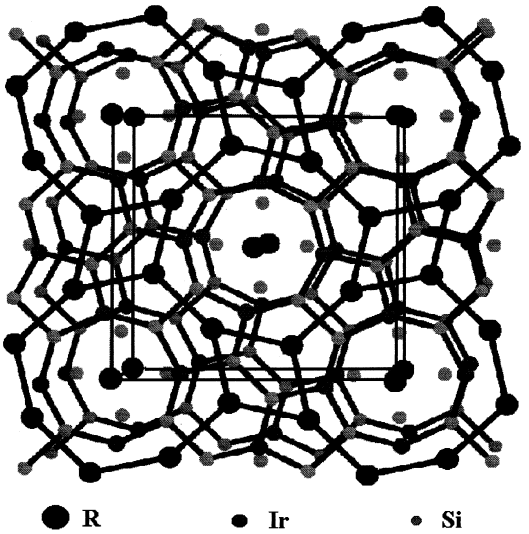

Figure 1. Structure of $Lu_5Ir_4Si_{10}$ (P4/mbm, $a = 12.4936$ Å, $c = 4.1852$ Å). Large, intermediate, and small spheres represent Lu, Ir, and Si, respectively. The Lu–Lu bonds shorter than 4.3 Å are indicated by the thick lines. Lu–Ir bonds have an intermediate thickness, and other bonds shorter than 3.3+ Åare drawn as thin lines. Lu(1) sites form a chain. Unit cell is also marked in the same figure.

3. Results and discussion

In what follows, we unequivocally establish the existence of CDW transition in $Lu_5Ir_4Si_{10}$ below 83 K and its coexistence with bulk BCS-type superconductivity below 3.9 K. The resistivity (ρ) and susceptibility (χ) data are shown in figure 2. Similar behavior is observed in χ(T) data (lower panel in figure 2). Both of them show sharp discontinuities (width $\approx$ 1.5 K) at 83 K (T_{CDW}) with small anisotropy. ρ exhibits normal linear T dependence above T_{CDW} but jumps to a higher value below T_{CDW} signifying the opening of a gap in the Fermi surface (FS). Similarly, the drop of χ at T_{CDW} implies loss in Pauli spin susceptibility due to CDW ordering. The rise in χ at low temperatures is due to the influence of magnetic impurities at the ppm level in 'pure' Lu used for making the sample. One can also observe that there is marked thermal hysteresis in both ρ and χ data from 65 to 70 K. Similar thermal hysteresis has also been seen (although the transitions are broad) in CuV_2S_4 which is attributed to multiple CDW transitions [5]. However, unlike CuV_2S_4, $Lu_5Ir_4Si_{10}$ becomes a superconductor below 3.9 K which can be seen in the ρ data.

Figure 3 shows the heat capacity (C_p) data between 2 K and 100 K. C_p shows a huge peak at T_{CDW} (ΔC_p=160 J/mol K) which is also very sharp. To the best of our knowledge, such a narrow and huge anomaly in C_p has not been seen in any CDW system including canonical CDW examples such as $NbSe_3$ or $NbSe_2$. The entropy involved in the CDW transition in $Lu_5Ir_4Si_{10}$ crystal is estimated to be $0.6R$ where R is the universal gas constant ($R =$ 8.314 J/mol K). The magnitude of the latent heat associated with this transition could not be observed in our experiment which could be either due to the low resolution ($\sim$ 1%) of our

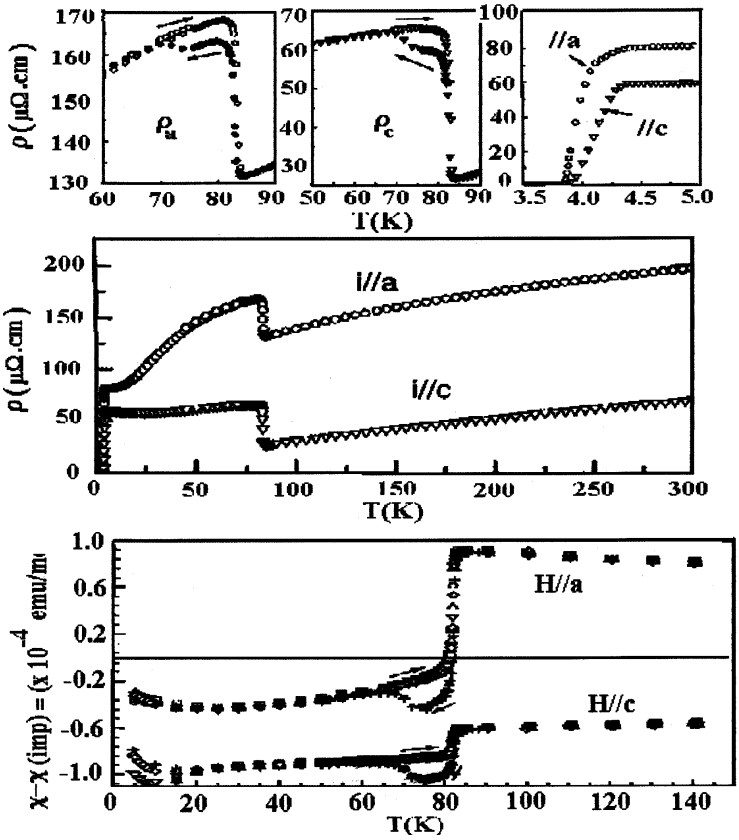

Figure 2. Panel (a) shows the variation of resistivity $\rho(T)$ of $Lu_5Ir_4Si_{10}$ along a- and c-axes from 2 K to 300 K. The insets show the CDW and superconducting transitions at 83 K and 3.9 K, respectively. Lower panel shows the temperature dependence of the susceptibility along a- and c-axes.

heat capacity set up or absence of any latent heat. At low temperatures, we observe another jump in C_p (at 3.9 K) (lower panel in figure 3) which confirms bulk superconductivity and this is in agreement with resistivity and susceptibility data. Below 3.5 K, the C_p data could be fitted to a standard BCS expression and the energy gap (Δ) is estimated to be around 7 K with the electron–phonon coupling constant (λ) equal to 0.43. Clearly, this indicates that $Lu_5Ir_4Si_{10}$ is a simple BCS superconductor which coexists with CDW ordering below 3.9 K.

A strong justification for CDW would be the observation of super lattice structure below the transition. Such a structure is indeed observed using single crystal X-ray diffraction and the temperature dependence of the fundamental peak (0, 0, 6) and the super lattice peak (0, 0, 5 + 3/7) from 2 to 100 K is shown in figure 4. The super lattice peaks are observed along c-axis below 80 K in the $(h, 0, l)$ plane. They can be indexed as $(h, o, l + q)$ where $q = m/7$ and $m = 1, 2, 3, 4, 5, 6$. This implies a commensurate lattice structure with seven

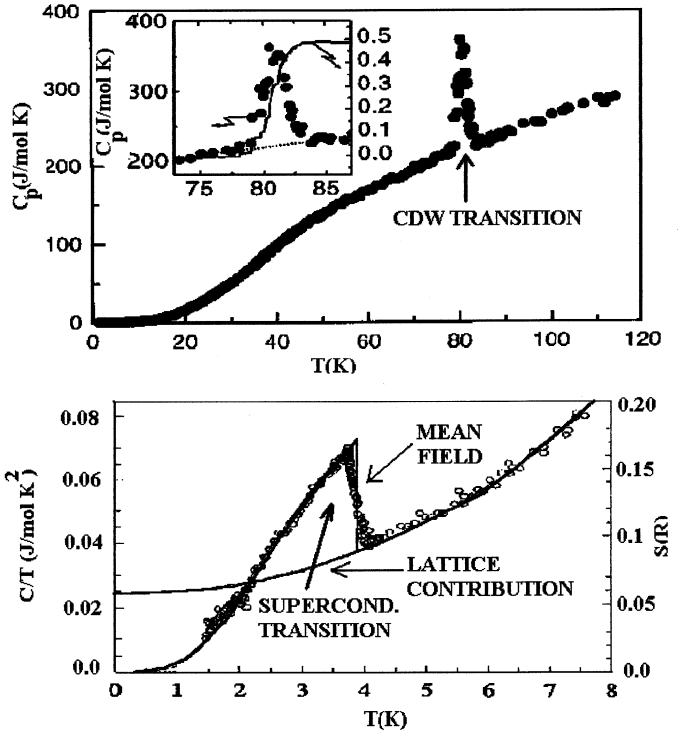

Figure 3. Plot of the heat capacity (C_p) of single crystal $Lu_5Ir_4Si_{10}$ vs. temperature (T) from 2 to 90 K. One can clearly see the two bulk transitions, namely, CDW ordering and superconductivity below 83 K and 3.9 K, respectively. The inset shows the entropy change at the CDW transition. The lower panel shows the C_p data at low temperatures where a BCS-type superconductivity is found to coexist with CDW.

unit cell period along c-axis. Although the fundamental period of modulation seems to be $q = 3/7$, the actual structural modulation is not a simple sine wave because of the presence of higher harmonics. Details of this analysis will be published elsewhere. The presence of the super lattice peak down to 2 K reaffirms the coexistence of CDW ordering [13,14] with superconductivity in $Lu_5Ir_4Si_{10}$ below 3.9 K.

In the case of a high quality single crystal of $Er_5Ir_4Si_{10}$, we first observe a combined commensurate structural transition and an incommensurate CDW (155 K), that locks into a purely commensurate state at lower temperatures (55 K), and local moment antiferromagnetism (below 2.8 K). This compound is iso-structural to $Lu_5Ir_4Si_{10}$. As opposed to earlier canonical CDW systems, the anomalies of the bulk properties at the 155 K CDW transition are much sharper in $Er_5Ir_4Si_{10}$. Thus, we believe that $Er_5Ir_4Si_{10}$ provides a unique opportunity to study local-moment magnetism, strongly coupled CDW and their interplay in the same compound. The long-range magnetic ordering is clearly seen in the bulk properties (see below) and in neutron diffraction [15]. Powder X-ray diffraction measurements showed that the samples have a tetragonal structure (see figure 1) and the lattice parameters are $a = 13.912(1)$ Å and $c = 4.591(1)$ Å.

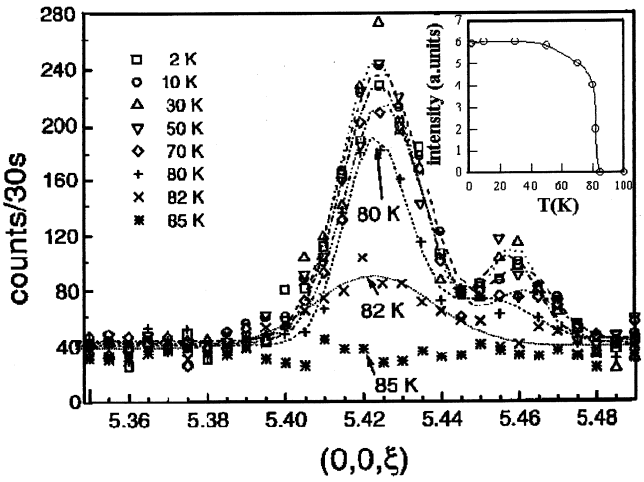

Figure 4. Temperature dependence of the fundamental peak (0, 0, 6) and super lattice peak (0, 0, 5 + 3/7) from 2 to 100 K from the X-ray diffraction measurements on the single crystal of $Lu_5Ir_4Si_{10}$.

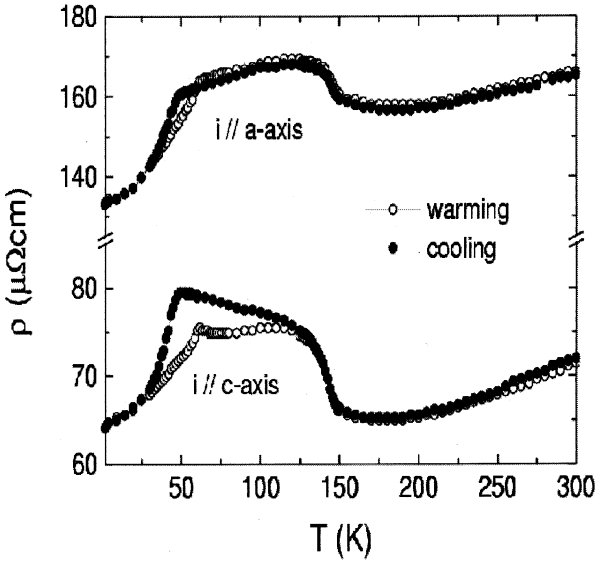

Figure 5. Temperature dependence of resistivity (ρ) of $Er_5Ir_4Si_{10}$ with current along a- and b-axes from 1.8 to 300 K. The sharp jumps reflect the two CDW transitions as explained in the text.

Figure 5 shows the temperature dependence of the resistivity between 1.8 K and 300 K along the a- and c-axes. An abrupt increase in ρ is observed at 155 K which, upon further cooling, develops into a plateau and drops sharply around 55 K. The dramatic changes in

$\rho(T)$ clearly elucidate the presence of two transitions at 155 K and 55 K. The pronounced hysteresis observed between 40 K and 120 K establishes the first-order character of the 55 K transition. Note that the anisotropy in the resistivity is quite small (2.4). This ratio is indeed much less than that observed in canonical CDW systems, such as $NbSe_3$. Low anisotropy indicates strong inter-chain. The behavior of $\rho(T)$ could be understood in terms of two conducting channels, one related to the Er1 sites and the other due to the Er2Er3 network. The first channel undergoes a metal–insulator transition at 155 K while the networks have finite conductivity that remains at all temperatures. Below the lock-in transition ($T = 55$ K), the commensurate modulation destroys the perfect nesting and ρ suddenly drops at this temperature. The magnetic susceptibility $\chi(T)$ obeys a simple Curie–Weiss law from 20 K to 300 K with an effective local moment of $\mu_{\text{eff}} = 9.7\mu_{\text{B}}$ and a Curie–Weiss temperature $\theta_p = 3.0$ K (data not shown). No anomaly is found at the temperatures of the CDW transitions. This is explained by the large local moment contribution to the susceptibility, that overwhelms any changes in the Pauli paramagnetism, as were observed in $Lu_5Ir_4Si_{10}$. The low temperature susceptibility data exhibit a peak at 2.8 K, thereby establishing the antiferromagnetic ordering of Er^{3+} moments below this temperature.

Figure 6 presents the specific-heat data between 2 K and 160 K of the same crystal. A huge peak in specific heat ($\Delta C_{\text{p}} = 160$ J/mol K) is observed at 145 K (see upper inset of figure 6) while no anomaly is found at the lower transition (55 K). The sharp [$(\Delta T/T_{\text{CDW}}) \sim 3\%$] upper transition is accompanied by a large entropy change of $0.6R$ where R is the gas constant. This suggests strong electron–phonon coupling in this phase transition which could arise due to a contribution from phonon softening that results in a Kohn anomaly [16]. In our earlier work we have established the occurrence of such a strong coupling CDW in the iso-structural compound $Lu_5Ir_4Si_{10}$ [17] where the gap is estimated

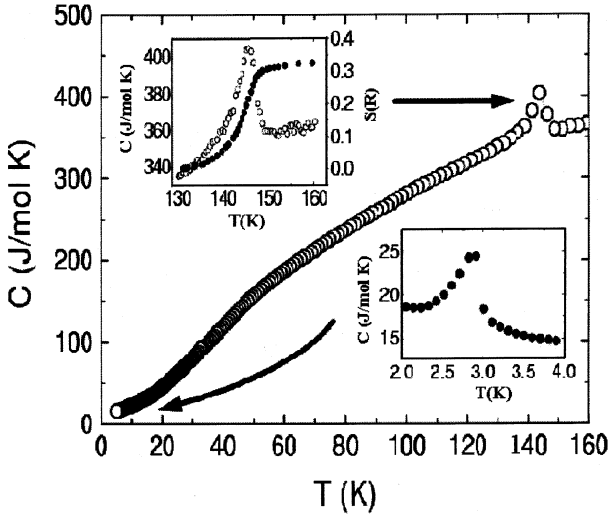

Figure 6. Temperature dependence of the specific heat (C_{p}) of $Er_5Ir_4Si_{10}$ from 2 to 160 K. The upper inset shows the behavior of C_{p} at the upper CDW transition along with the entropy estimated after the background subtraction. The lower inset displays the specific heat data below 4 K.

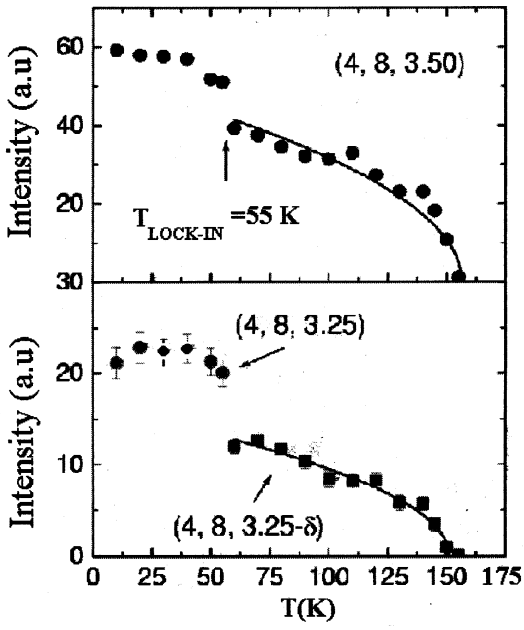

Figure 7. Intensities vs. temperature for the satellite reflections (4, 8, 3.50), (4, 8, 3.25-δ) and half of the intensity of (4, 8, 3.25) [(4, 8, 3.25 + δ) not shown] from a Q-scan. The lines show a $(T_c - T)^{1/2}$ dependence.

to be around 700 K indicating that the actual phase transition is suppressed well below the mean-field value. A similar scenario is very likely applicable to $Er_5Ir_4Si_{10}$. The sharp ($\Delta C_p = 10$ J/mol K) specific-heat anomaly at 2.8 K, shown in the lower inset of figure 6, reflects the bulk nature of the magnetic transition. Moreover, the transition could be easily suppressed by applying a magnetic field of 1 T (data not shown). High-resolution X-ray diffraction on a small homogeneous piece of single crystal was performed with synchrotron radiation for temperatures between 10 K and 300 K. Below $T_c = 155$ K, five superlattice reflections start to develop along c^* between consecutive Bragg reflections. Upon cooling, the intensities of these reflections increase, and hysteresis was not observed, suggesting a second-order transition at 155 K (figure 7). In accordance with this interpretation, the temperature dependence of the intensities of the superlattice reflections is proportional to $(T_cT)^{1/2}$. However, due to the large scattering of the data points, our experiment does not allow an accurate determination of the critical exponent. The positions of these reflections can be described by modulation wave vectors $q_1 = (0, 0, 1/4\delta)$, $q_2 = (0, 0, 1/4 + \delta)$ and $q_3 = (0, 0, 1/2)$. Figure 7 illustrates the development of the incommensurate peaks beginning at 155 K and merging into a commensurate $q = (0, 0, 1/4)$ single peak at 55 K. The inset of figure 7 displays the incommensurability δ which clearly depends continuously on the temperature and, thus, indicates a truly incommensurate CDW state. At 55 K a lock-in transition is observed, whereby δ jumps to zero, and a 4-fold superstructure results. The lock-in transition is seen as a small increase of the intensity of the (0, 0, 1/2) satellite, as shown in the upper plot of figure 6. Furthermore, the intensity of the (0, 0, 1/4) satellite

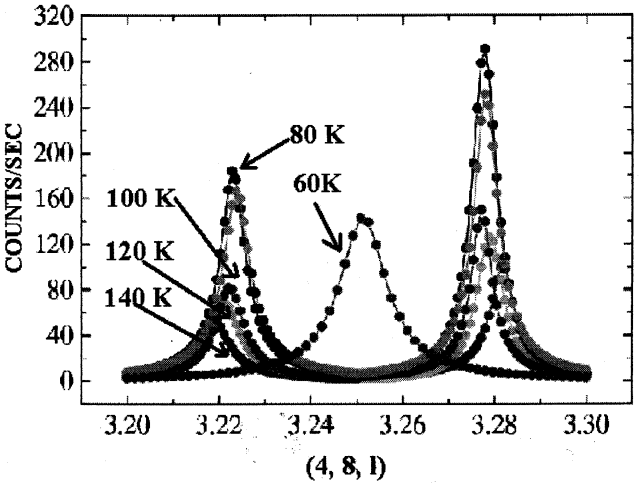

Figure 8. Temperature dependence of the Q-scan X-ray reflections (4, 8, [3.20 . . . 3.30]). The two peaks coming from the incommensurate component merge into a single peak in the commensurate state at 55 K. The inset shows the temperature dependence of the incommensurability δ (as defined in the text).

($\delta = 0$), as found from the Q-scan experiment, just below T lock Γ in is approximately equal to the sum of the intensities of the corresponding incommensurate satellites at (0, 0, 1/4 $\Sigma\delta$) just above T lock Γ in. The simultaneous development of incommensurate and commensurate modulations makes $Er_5Ir_4Si_{10}$ an atypical CDW system. Two scenarios can be envisaged to explain this feature. In the first, it is assumed that at T_c the unit cell doubles. The Fermi surface is modified accordingly and allows nesting resulting in a 1D-incommensurate CDW where $q_{1D} = (0, 0, 1/22\delta)$ with respect to the doubled unit cell. We note that a transition towards a structure with a doubled c-axis is possible via a second-order phase transition [18]. Therefore, we propose that the transition at $T_c = 155$ K, is a second-order, structural phase transition. The modified electronic structure then induces the CDW transition, whereby the order parameter of the CDW grows in concert with the order parameter of the structural transition. The CDW state might be favored in the doubled unit cell by a better nesting condition or by an increased electron–phonon coupling. Polycrystalline and single crystal neutron data suggest the presence of a large magnetic moment on the Er1 site and smaller ones on Er2 and Er3 sites, below 2.8 K [15]. The presence and interaction of local moments in this material classify $Er_5Ir_4Si_{10}$ as the first intermetallic CDW system with local moment ordering. Although it is possible to understand the behaviors of ρ and χ within the CDW and local moment pictures, the large peak in the C_p at 145 K denotes this CDW transition as an unusual one, unlike conventional CDW systems where the anomalies in the bulk properties are quite weak at the transition. It is generally believed that defects tend to wipe out the sharp anomaly in conventional CDW compounds. In stoichiometric single-crystal $Er_5Ir_4Si_{10}$, we expect that the influence of defects will be much smaller making this system essentially disorder free. One does not observe any anomaly in C_p around 55 K since it is a lock-in transition, which probably

involves very small entropy change but a large change in the resistivity due to the decrease of the energy gap.

4. Conclusion

In conclusion, we have established that $Er_5Ir_4Si_{10}$ exhibits multiple CDW transitions (1D-incommensurate at 155 K and lock-in at 55 K) and a transition towards a magnetically ordered state at 2.8 K. We speculate that the magnetic moments of the Er atoms play a definite role in these transitions and further understanding requires band structure calculations to determine the possible nesting and gapping of the Fermi surface which leads to the CDW transitions [19]. Finally, we would like to stress that the $R_5Ir_4Si_{10}$ series offer a new and extremely convenient paradigm with which to study strong coupling CDW and coexisting superconductivity or magnetism.

Acknowledgement

This work was done in collaboration with Prof. J Mydosh's group at Kamerlingh Onnes Laboratory, Leiden, The Netherlands.

References

[1] See Chapters in *Electronic properties of quasi-one dimensional materials* edited by P Monceau (Reidel, Dordrecht, The Netherlands, 1985)
[2] G Gruener, *Charge density waves in solids* (Elsevier Science Publishers, North Holland, Amsterdam, 1996)
[3] H F Braun, *J. Less Common Metals* **100**, 105 (1984)
[4] G Gruebel *et al*, *Phys. Rev.* **B43**, 8803 (1991)
[5] T Sekine *et al*, *Solid State Commun.* **51**, 187 (1984)
Y Koshimoto *et al*, *Solid State Commun.* **96**, 23 (1995)
[6] Shiyou Pei *et al*, *Phys. Rev.* **B39**, 811 (1989)
[7] R N Shelton, L S HausermannBerg, P Klavins, H D Yang, M S Anderson and C A Swenson, *Phys. Rev.* **B34**, 4590 (1986)
[8] H D Yang, P Klavins and R N Shelton, *Phys. Rev.* **B43**, 7688 (1991)
[9] K Ghosh, S Ramakrishnan and Girish Chandra, *Phys. Rev.* **B48**, 4152 (1993)
[10] H F Braun, *Acta Crystallogr.* **B36**, 2397 (1980)
[11] H F Braun and C U Segre, in *Ternary superconductors* edited by G K Shenoy, B D Dunlap and F Y Fradin (North Holland, Amsterdam, 1980) p. 239
[12] H D Yang, R N Shelton and H F Braun, *Phys. Rev.* **B33**, 5062 (1986)
[13] W L McMillan, *Phys. Rev.* **167**, 331 (1968)
[14] G Bilbro and W L McMillan, *Phys. Rev.* **B14**, 1877 (1976); see also C A Baleseiro and L M Falikov, in *Superconductivity in d- and f-band metals*, edited by H Suhl and M B Maple (Academic Press, New York, 1980) p. 105
[15] F Galli, S Ramakrishnan, T Tanugichi, G J Nieuwenhuys, J A Mydosh, S Geupel, J Ludecke and S Van Smaalen, *Phys. Rev. Lett.* **85**, 159 (2000)
See also F Galli, R Feryernherm, S Ramakrishnan, G J Nieuwenhuys and J A Mydosh, *Phys. Rev.* **B62**, 13840 (2000)

[16] D E Moncton, J D Axe and F J DiSalvo, *Phys. Rev. Lett.* **34**, 734 (1975)
[17] B Becker, N G Patil, S Ramakrishnan, A A Menovsky, G J Nieuwenhuys and J A Mydosh, *Phys. Rev.* **B59**, 7266 (1999)
[18] H T Stokes and D M Hatch, *Isotropy subgroups of the 230 crystallographic space groups* (World Scientific, Singapore, 1988)
[19] Very recently dissimilarities were drawn between conventional CDW systems, e.g., $TaSe_2$ [R M Fleming, D E Moncton, D B McWhan and F J Di Salvo, *Phys. Rev. Lett.* **45**, 576 (1980)], and the charge ordered perovskite manganites [C H Chen, S Mori and SW Cheong, *Phys. Rev. Lett.* **83**, 4792 (1999)]. It would be particularly interesting to contrast the charge and spin orderings in RE5 Ir4 Si10 with these latter oxides.